



Microseism oscillations: from deterministic to noise-driven models

Vladimir B. Ryabov ^{a,b,*}, A.M. Correig ^c, M. Urquizu ^c, A.A. Zaikin ^d

^a *Department of Complex Systems, Future University Hakodate, 041-8655 Hakodate, Hokkaido, Japan*

^b *Department of Microwave Electronics, Institute of Radio Astronomy, 61002 Kharkov, Ukraine*

^c *Departament d'Astronomia i Meteorologia, Universitat de Barcelon, E-08028 Barcelona, Spain*

^d *Institute of Physics, Potsdam University, D-14469 Potsdam, Germany*

Accepted 30 May 2002

Abstract

Microseism time series, recorded in a broadband seismic station located at the eastern Pyrenees, 50 km far from the Mediterranean Sea, have been analyzed by means of the dynamical system tools in an attempt to elucidate whether the recorded time series are linear or nonlinear, deterministic or stochastic. We have detected strong evidences that microseism time series are stochastic, and no evidence of nonlinearity and/or determinism has been found. In order to get more insight on the underlying mechanism, we tested a toy model that reproduces some observable characteristics of the microseisms. This toy model consists in a forced, damped nonlinear oscillator in which the force term is composed of two harmonic forces and additive white noise. We have concluded that noise contribution is of fundamental importance in modeling the spectral properties of observed time series, and assimilate it to the ubiquitous local, high frequency noise. A global mechanism for microseism generation is suggested in terms of atmospheric turbulence at different wavelengths.

© 2002 Elsevier Science Ltd. All rights reserved.

1. Introduction

Steady unrest of the ground detected by seismometers located virtually anywhere in the world is usually called microseism oscillations. It should be noted, that these ground motions are not related to any earthquake activities nearby, and are interpreted as a strong background noise in the records of seismic waves generated by earthquakes. The early studies of the spectral characteristics of microseisms [1] revealed two distinct maxima in their power spectra, at about 0.1 and 0.2 Hz, typically present in almost all the records performed at different seismic stations. The lower peak is located at about 0.1 Hz and has been interpreted as a direct result of the oscillations generated by ocean waves on nearby coasts, since its shape and frequency position as a rule coincides with the main peak in the spectrum of the ocean waves. The interpretation for the highest one had been first proposed by Longuet-Higgins [2] in terms of nonlinear wave transformation mechanism. The basic idea suggested in [2] can be briefly summarized as follows. Two gravity waves of approximately the same periods propagating in opposite directions on the surface of the ocean can give rise to the pressure variations at the seabed. These oscillations can produce acoustic disturbances that have the peak in the power spectrum at about twice the characteristic frequency of the two ocean gravity waves and propagate through the solid earth as surface waves, mainly of Raleigh type. The current state of the art in the field of microseisms data and analysis is given in the review by Webb [3].

* Corresponding author. Address: Department of Complex Systems, Future University Hakodate, 041-8655 Hakodate, Hokkaido, Japan.

The presence of two maxima in the power spectrum of microseism oscillations is a characteristic feature of the background seismic noise. Their location on the frequency axis can be slightly changed depending on the place where the record had been obtained, but the approximate ratio 2:1 seems always be the case. As for the magnitude of microseism oscillations, its variation is rather big (about two orders of magnitude), depending on either the location of the seismic station or the power of the sea storm somewhere nearby.

In Fig. 1a we show two parts of different microseism time series recorded at the broadband seismic station CAD located at the eastern Pyrenees, at about 50 km from sea [4] for a quiet day (bottom) and for a stormy day (top). Fig. 2 displays their corresponding power spectra with distinct peaks at ~ 0.06 and ~ 0.11 Hz. Following Webb [3], we can interpret these spectral peaks as those corresponding to teleseismic microseisms, whereas that of ~ 0.016 Hz to infragravity waves. The small peaks located between 0.4 and 2 Hz correspond to local seismicity, and the signal located at frequencies higher than 2 Hz to local seismic noise.

So far, the spectral study of microseism records has been mainly used for the analysis and interpretation of the background seismic noise. This means that linear theory of waves propagation and transformation was the principal tool utilized for this purpose [5]. At the same time, it has been well established that the basic mechanism responsible for the appearance of microseisms should be intrinsically nonlinear interaction of two ocean waves [3,6]. If to accept as the working hypothesis that nonlinear wave transformation plays a key role in generating microseisms, an interesting question appears of whether it is possible that deterministic chaos can be responsible for the apparent complexity observed in the microseism records. In this article we would like to address this question in detail and also discuss in quantitative terms the degree of nonlinearity present in microseism records as well as the role of stochastic (noise) components in the data and mathematical models traditionally used in the analysis. In this work, the hypothesis of the deterministically chaotic origin of microseisms is tested against the alternative ones based on the assumption of a purely stochastic nature of the recorded oscillations. In the framework of such alternative considerations, the wide spectral peak in microseism records can be either the manifestation of frequency selective properties of the source generating the elastic waves or the result of propagation effect, when initially excited noise-like envelope of elastic waves is transformed in the solid earth waveguide playing the role of a (maybe nonlinear) filter.

In our investigations, we accept the classification scheme of complex time series, similar to the one proposed by Palus [7], that enables one to elucidate the physics of microseism generation mechanism. We test three possibilities for designing a general model, capable of reproducing the observed waveforms of microseism oscillations.

1. Nonlinear deterministic
2. Linear stochastic
3. Nonlinear stochastic

The comparison between the models is carried out by calculating a set of measures known as discriminating statistics (DS). DS are defined as quantitative measures of the data series based on some of their statistical properties. The classification of the recorded time series is performed by comparing the same DS for original data and so called surrogates. Surrogates are computer generated time series obtained from the original data by specially designed algorithms, suppressing some specific properties of the data, while preserving other characteristics intact. The necessity of exploiting such method for classifying the results of numerical analysis comes from our inability to estimate confidence intervals for some DS, like correlation dimension or other indicators of determinism and/or nonlinearity present in the data. The availability of many computer generated surrogate time series allows calculating the probability distribution function for any given DS, with subsequent error estimation by standard statistical methods.

For obtaining the surrogates, we used the following techniques:

- (a) randomization of phases of the Fourier transform (RP),
- (b) autoregressive moving average model (ARMA),
- (c) nonlinear quasi-periodically forced oscillator with and without additive noise terms (NLFO-N, NLFO).

The description of RP and ARMA methods can be found in many works (see e.g., [8,9] and references therein), so we do not reiterate it here. As for the NLFO model, the detailed discussion of this model can be found in Section 3.

The calculation of the same DS has been performed for both the available data records and their surrogates, thus allowing choosing between the three types of models given above. Besides using the standard measures like correlation dimension, we also studied linear and nonlinear redundancies, local prediction properties, and DS of instantaneous amplitudes based on the Hilbert transform of the time series. Comparative analysis of all those techniques enabled us to perform (sometimes very subtle) distinction between different classes of nonlinear models consistent with the available data.

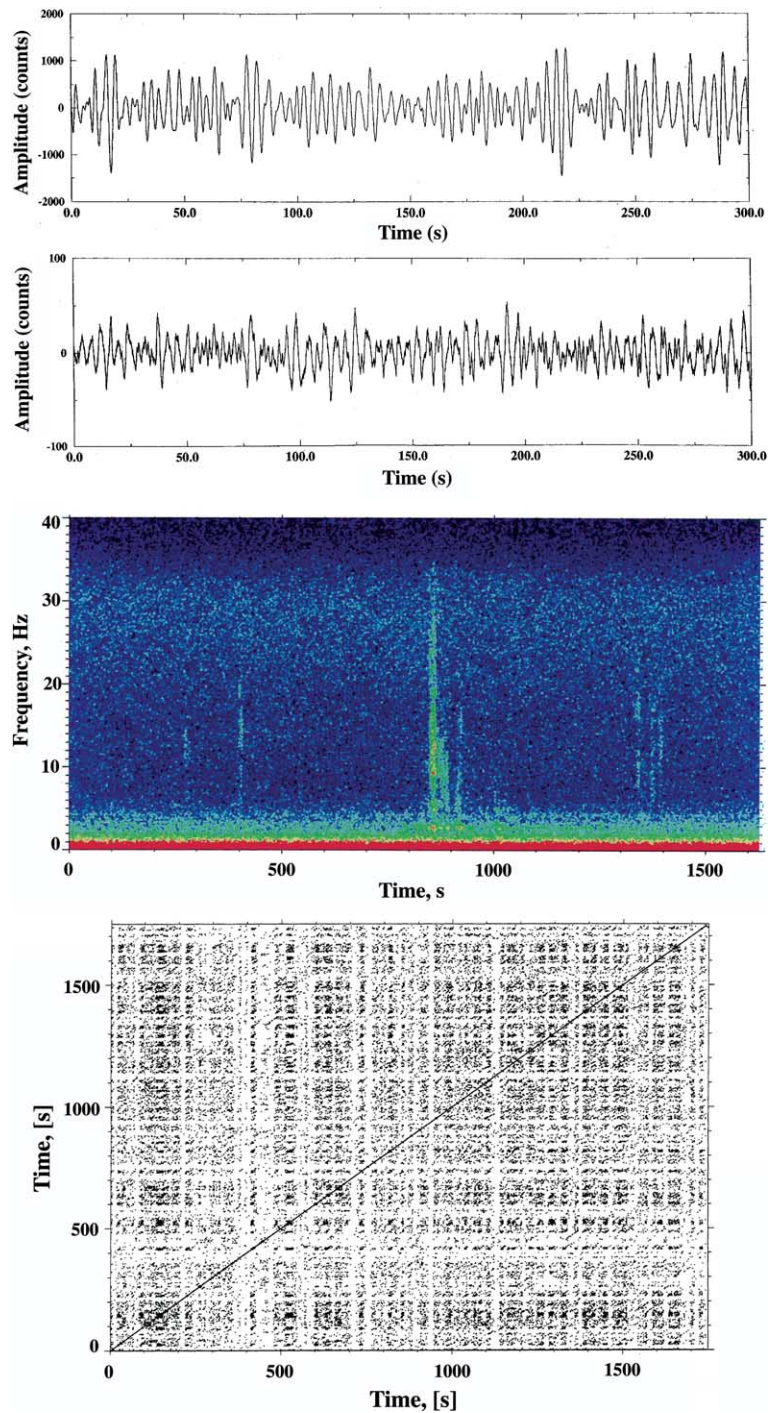


Fig. 1. (a) Examples of high amplitude (top) and low amplitude (bottom) microseism records (vertical component). Note the difference in the amplitude scale. (b) Dynamic spectrum and recurrence plot (c) for the high amplitude microseism signal. In the calculation of the recurrence plot 14-dimensional embedding space and the delay time 0.5 s are used.

The overall procedure of our data analysis is as follows. First, we perform a standard Fourier and autocorrelation analysis of the time series in order to estimate the characteristic time scales present of the data. At this stage, we also carry out preliminary data processing consisting in filtration of additive noise and test the stationarity of the time series.

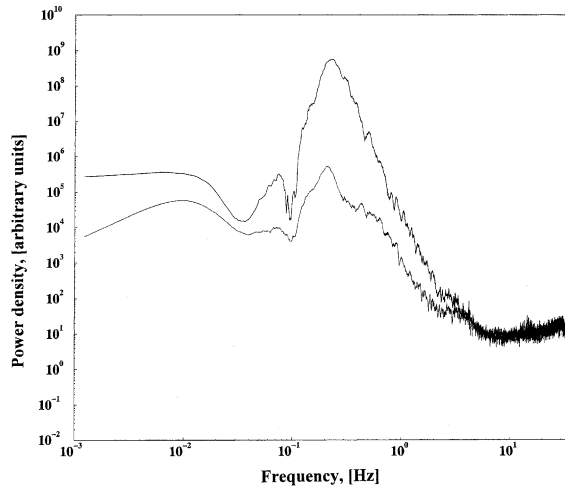


Fig. 2. Power spectra of the high and low amplitude microseisms.

This stage is accomplished by calculating mutual information [10] for obtaining the value of characteristic time scales of information decay in the data and plotting the return maps for getting a rough representation of the nonlinear dynamics underlying the studied process. Next, we calculate the correlation dimension for the microseism series, and, in the case of detecting its finite value, repeat the procedure with surrogate time series. As noted by many authors, even if DS for surrogates are statistically different from the ones calculated for the original time series, other additional tests are necessary to support or reject the hypothesis about chaotic nature of the data. Therefore, we also perform the calculation of redundancies [7], local prediction models [11], and, finally, statistical distribution of instantaneous amplitudes [12] to get additional evidence in favor of (or against) the hypothesis on the presence of deterministic components in the data. Surprisingly enough, no decisive evidence for nonlinearity or determinism has been found in the analyzed time series. This result justifies the necessity of considering stochastic or noise-driven systems as alternative models consistent with the available microseism data.

The paper is organized as follows: A brief description of our numerical experiments and data processing methods is given in Section 2. In Section 3 a toy model utilizing noise as a driving force is proposed that generates time series with spectral characteristics similar to microseism data. In Section 4 we discuss the obtained results and possible global mechanisms for microseism generation.

2. Analysis of microseism time series

The following describes the tests we ran on the observed time series. For more details of the methods and algorithms discussed in the present work see e.g., [8,10–15] and references therein.

2.1. Dynamical tests

2.1.1. Stationarity

Many physical phenomena can be described in terms of statistical equilibrium, that is, if we take into consideration a given interval of a time series and divide it into subintervals, the distinct sections appear “the same”. More precisely, we can say that the statistical properties of the stationary process (the moments of different order) are independent of time. It should be noted that the property of stationarity is crucial for subsequent calculations of dynamic invariants, like correlation dimension or redundancy. That is why considerable efforts have been made in order to suppress nonstationary components present in our data. Besides applying traditional statistical procedures of moments calculation and Chi-square tests [16], we also used the analysis based on visual inspection of spectrograms and recurrence plots [17]. The former one (also called windowed Fourier transform) may be considered as a traditional tool for visualizing nonstationarities displayed by different Fourier components of the power spectrum. A conventional way of visualizing Fourier content of complicated waveforms is to plot two-dimensional dynamic spectra, with time along the abscissa and frequency along ordinate. In such a presentation, the color indicates the intensity of corresponding Fourier component.

Usually the interference patterns, like man generated signals or earthquakes, can be easily recognized on such two-dimensional plots and filtered out before subsequent processing.

2.1.2. Autocorrelation

The autocorrelation function of a linear process is a measure of the degree of dependence that is present in the values of a time series $s(t)$, delayed by an interval τ , known as delay time. For a random process, the autocorrelation function fluctuates randomly around zero, indicative of a lack of memory of a given time with respect to the past. For a periodic process, the autocorrelation function is also periodic, indicative of a close relation between values that repeat on time. The first zero crossing of the autocorrelation function is a measure of the time for which data become independent. This time is also of interest in dynamical systems theory since it provides a criterion for selecting the delay time in the procedure of phase space reconstruction.

The coherence time t_0 of the autocorrelation function is the time for which the absolute value of the autocorrelation is lower than a given h for all $t > t_0$. If the autocorrelation function vanishes exponentially for $t \rightarrow \infty$, the coherence time is finite, and otherwise infinite. A large coherence time, of the order of the length of the analyzed time series, may be indicative of nonlinearity.

2.1.3. Embedding

Most of the recently proposed techniques for finding determinism and/or nonlinearity in experimental time series are based on the celebrated embedding theorem by Takens [18] stating that it is possible to extract certain information about the multidimensional dynamical system used as a mathematical model of the studied phenomenon from a scalar time series corresponding to the temporal evolution of a single coordinate. In particular, the theorem states that such dynamic invariants as fractal dimension of the underlying attractor or Lyapunov characteristic exponents can be calculated by analyzing the statistical properties of the reconstructed multidimensional trajectory in the phase space. The commonly accepted procedure for the study of dynamical invariants uses time-delayed copies of the scalar time series as the components of multidimensional vectors in the reconstructed phase space and analyzes the dependence of the invariants on the dimensionality of the phase space. In the case of sufficiently long and clear from noise time series, such a procedure allows discriminating between deterministic and stochastic processes and detecting the presence of deterministic chaos in the experimental data.

2.1.4. Recurrence plots

It is a useful tool for displaying hidden correlations in the data resulting from quasi-regular behavior of phase trajectories, recurrences to any point in the reconstructed n -dimensional phase space. If the dynamics of the system is deterministic (periodic or chaotic), phase trajectory evolves in a similar manner in any small area of the phase space, that is a manifestation of smoothness of underlying dynamical system. This property can be analyzed by monitoring the local statistics of phase trajectories in some preselected areas of phase space. Technically, it is performed by finding all the neighboring points $x_j(r)$ within a predefined distance r around each point x_i of the data. Then, the time position j of all the neighbors is plotted against the time position of the reference point i . In the case of deterministically evolving system, these plots present quasi-regular patterns and can be used both for the purpose of discriminating chaotic processes from noise and detecting nonstationarities in the data [17,19]. In particular, approximate symmetry of recurrence patterns with respect to the main diagonal serves as the indication of stationarity of the studied process, while the appearance of clusters is a feature of determinism.

2.1.5. Mutual information [10]

Let x and y be two random variables (or, equivalently, two samples $s(t)$ and $s(t + \tau)$ of a time series). The mutual information provides us with the amount of information that the variable y contains on the variable x . The mutual information is computed in terms of Shannon entropy and can be viewed as a nonlinear generalization of the autocorrelation function. If two samples are independent, the mutual information is zero. For a time series, the first local minimum in the plot of mutual information versus delay time is considered as better estimate for the optimal time delay compared to the first zero crossing of the autocorrelation function (which is defined for linear processes).

2.1.6. Redundancy

Constitutes an extension of the mutual information (which is defined for two-dimensions (variables)) to m -dimensions (variables). One should distinguish between *general* (or nonlinear) and *linear* redundancy. The linear one is computed from the correlation matrix of a given time series and constitutes a characterization of linear properties of the data in terms of linear dependence (correlation) between n -components of the reconstructed phase trajectory in the m -dimensional phase space. On the other hand, the amount of (possibly nonlinear) common information contained in the

m -components is called general redundancy and is a useful measure for detecting a general type of dependence between variables. It has been proposed by Palus [7] to use differences in the plots of linear and general redundancy as indicators of the presence of nonlinearity in the data. In this approach, both redundancies are calculated and plotted as functions of time delay between the components of the reconstruction phase space. Palus has shown that in the case of deterministically chaotic nonlinear systems, significantly different shapes of the linear and general redundancy curves are observed, like e.g., different number of and/or time lag position of maxima, absence or presence of various trends, etc. Thus, if by comparing linear and general redundancy plots we observe significantly different structures the presence of nonlinearity can be suspected.

2.1.7. Correlation dimension [20]

The dynamics of a dissipative deterministic system is defined by the geometry of the attractor in the phase space (the region where a dissipative system evolves once the transients have vanished). If the attractor is of low dimension the system is deterministic, otherwise it is, or behaves as, stochastic. The correlation dimension gives a good approximation to the attractor's dimension, computed from the *correlation integral*. The correlation integral $C_m(r)$ is defined as the fraction of all pairs of points on the reconstructed attractor separated by distances less than r . It is usually computed for a chosen range of distances r in the phase spaces of increasing dimension m . The power law dependence of the correlation integral on r

$$C_m(r) \sim r^{\nu_m}$$

enables one to calculate the exponents ν_m in the limit $r \rightarrow 0$. The limiting value, ν (if it exists as $m \rightarrow \infty$) of the exponent ν_m is called correlation dimension and defines the minimal number of independent coordinates, necessary for describing the dynamics of the system. The plot of ν_m versus m shows saturation for a deterministic system at a value equal to ν , whereas the absence of apparent saturation is a characteristic feature of random processes. If the saturation is detected, the surrogate data test has to be applied. This approach allows testing the null hypothesis that the studied data belong to the class of linear stochastic Gaussian processes (which the surrogates belong to) against the alternative that the data are deterministically chaotic. By rejecting the null hypothesis, the conclusion about intrinsic determinism and/or presence of nonlinearity in the analyzed data can be derived [14].

2.1.8. Determinism versus stochasticity

This test consists in fitting a set of local prediction models to several subsets of data. The basic idea underlying this approach consists in the expectation to obtain better short-time prediction for deterministic (even chaotic) models compared to the stochastic ones. The procedure proposed by Casdagli and Weigend [11] is based on the Takens reconstruction of the phase space and linear approximation of the dynamics in small areas around (some of) the data points. The first half of the available data is then used as training set for computing linear predictors. The second half of the data is utilized for estimating the short-term predictive power of the predictors found from the analysis performed in the previous stage. By varying the size of the local neighborhood used in building the linear predictive models, one then analyzes the dependence of the predictive power (the error value $E(k)$) on the degree of locality (the number k of nearest neighbors used) of the model. If the error is smaller for fewer neighbors used (highly local models are effective), the data are concluded to originate from a deterministic process. If, on the contrary, large amount of neighbors give better prediction, the time series is a stochastic process.

2.1.9. Rytov–Dimentberg criterion

This criterion, not yet widely spread in the literature, was proposed by Rytov [21] and later by Dimentberg [22] as a tool to distinguish between noises passed through a filter from self-sustained oscillations with additive noise. The criterion has been further extended by Landa and Zaikin [12] for distinguishing filtered noise or noise-induced oscillations from chaotic self-sustained oscillations in the presence of noise. According to this criterion, the probability density for the *instantaneous amplitude* squared is a monotonously decreasing function, if the time series is obtained from filtered noise or noise-induced oscillations, whereas for self-sustained oscillations, even in the presence of intensive external noise, this function displays several well-pronounced peaks.

The instantaneous amplitude refers to the amplitude of *analytical signal* $z(t)$ constructed from the time series $s(t)$ with the use of Hilbert transform

$$h(t) = \frac{1}{\pi} \text{PV} \int_{-\infty}^{\infty} \frac{s(\tau)}{t - \tau}$$

where PV means the integral taken in the sense of the Cauchy principal value. This integral transformation is widely used in signal processing and provides a 90 degree phase shift of all the spectral components of the signal $s(t)$. In other

words, the Hilbert transformed signal $h(t)$ can be thought of as the imaginary component of the real signal, $s(t)$. Its instantaneous amplitude $A(t)$ is defined as $A(t) = \sqrt{s^2(t) + h^2(t)}$ and refers to the magnitude of analytic signal $z(t) = s(t) + ih(t)$ constructed from the time series $s(t)$ (see e.g., [23,24]). A practical way to apply this criterion simply consists in the construction and further analysis of histograms of the square of instantaneous amplitude for the observed time series $s(t)$.

2.2. Data analysis

Microseism time series have been selected from 30 min window seismograms recorded at CAD broad band station at a sampling rate of 80 Hz during 1995 and 1996, starting at 03:00 am to avoid cultural noise; for details see [4]. If some earthquakes (teleaseism or local) were present during this time window, the record was rejected. In total we have analyzed 40 time series corresponding to high microseism activity (high amplitude microseisms) and 15 time series of low microseism activity (low amplitude microseisms).

We have applied the tests briefly described in the previous section to the microseism time series with the following results (in the figures that follow, all examples correspond to the high amplitude microseism shown in Fig. 1).

2.2.1. Stationarity

Time series are stationary for time intervals longer than 350 s (roughly five times the period of the widest wave packet). Fig. 1 also shows examples of periodogram (b) and recurrence plot (c) for a high amplitude microseism record of December 27, 1995. The dynamic spectrum shows apparent short-time nonstationarities at about 250, 400, 860–920, 1350–1450 s, which may be caused by local events. Similar interpretation is also given in [3] (caption of Fig. 4). Prior to calculating correlation dimension or any other characteristics of nonlinearity/determinism, those parts have been filtered out. As for the recurrence plot, it shows no apparent inhomogeneity in the direction orthogonal to the diagonal, thus providing an additional support in favor of stationarity of the microseism data. At the same time, it presents some indication of nonlinearity, for the distribution of points shows certain structures that cannot be expected from a purely random time series.

2.2.2. Autocorrelation

The autocorrelation function displays the first zero crossing at about 1 s, that constitutes an estimate for the coherence time (see Fig. 3). We can distinguish two more characteristic time scales (coherency times), a finite one of about 15 s, where oscillations become stable, and another one, seemingly infinite, defined by an average value of the autocorrelation at the level ~ 0.1 . Fig. 3 displays the autocorrelation function for microseisms of both high and low amplitude, clearly showing that they share the same characteristics.

2.2.3. Mutual information and redundancy

Fig. 4 (top) displays the linear redundancy for the embedding dimensions $m = 2, 3, 4$, and (bottom) general redundancy, calculated at fixed values of all the control parameters. The curve for $m = 2$ (bottom) corresponds to the

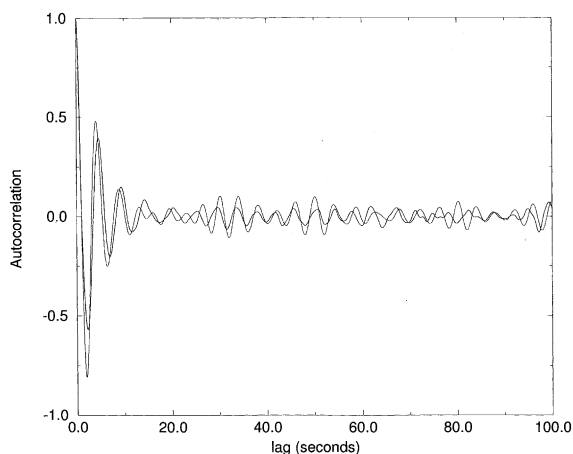


Fig. 3. Autocorrelation function of the high and low amplitude microseism shown in Fig. 1.

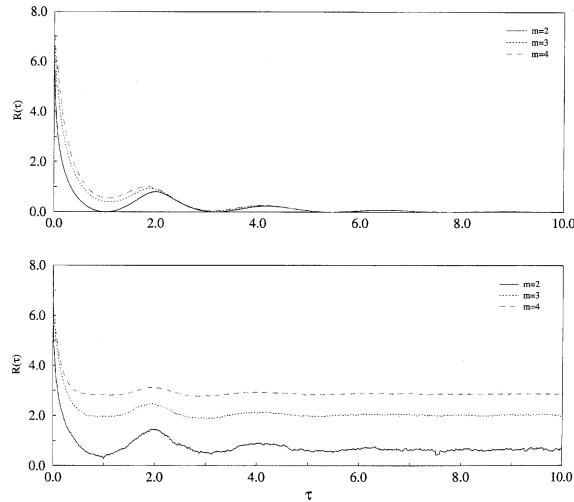


Fig. 4. Redundancies for the high amplitude microseism. Linear (top) and general, or nonlinear (bottom) redundancy plots for three values of the embedding dimension: $m = 2, 3, 4$. The nonlinear redundancy for the embedding dimension $m = 2$ corresponds to the mutual information.

mutual information. It presents a minimum at about 1 s, thus providing the good choice for the value of delay time in the Takens reconstruction procedure. For the three-dimensions shown, the structure of the redundancy curves is not significantly different (this behavior, not shown for clarity, continues up to $m = 10$), indicating the absence of determinism and nonlinearity in the analyzed time series.

2.2.4. Correlation dimension

Fig. 5 presents an example of local slope curves $D_m(r)$

$$D_m(r) = \frac{d[\log C_m(r)]}{d[\log r]}$$

calculated for a high amplitude microseism time series. It is shown in logarithmic coordinates for embedding dimension m changing from 2 to 11 and the delay time $\tau = 1$ s. Although the characteristic plateau is rather well defined for $m = 2$ and 3, its presence is not obvious for higher embedding dimensions. On the other hand, the inspection of these curves does not allow discarding the possibility of deterministic behavior, since the local slope of the correlation integral at small values of r is apparently less than the embedding dimension, especially at high values of the latter. Moreover, by applying some of the tests developed for this purpose in the literature [25], the finite value of correlation dimension can be surely detected for the curves shown in Fig. 5 corresponding to high embedding dimensions. Therefore, to make the final conclusion on the presence of determinism in the given data, we perform additional tests, e.g., those based on the analysis of surrogate time series.

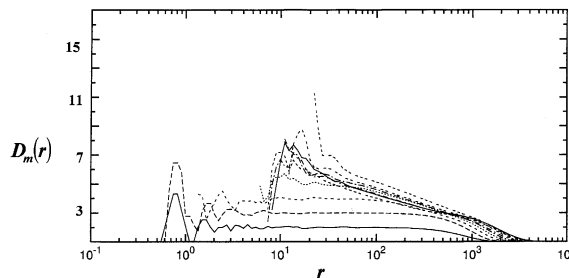


Fig. 5. Local slope of the correlation integral $C_m(r)$ versus the distance r for the embedding dimension changing from $m = 2$ to $m = 11$ for the high amplitude microseism time series.

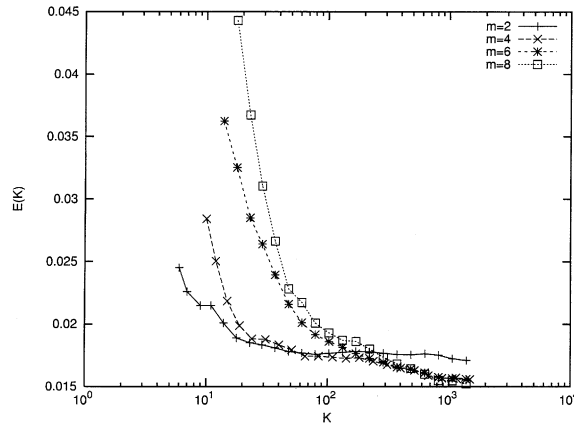


Fig. 6. DVS test for the high amplitude microseism. The dependence of normalized prediction error $E(k)$ on the cluster size (number of points k) used in deriving the linear predictors in the reconstructed phase space.

2.2.5. Determinism versus stochasticity

Fig. 6 presents the example of applying the determinism versus stochasticity (DVS) test to a microseism series for embedding dimensions $m = 2, 4, 6, 8$ (results are independent of the time delay used). For all the dimensions, the prediction error is a decreasing function of the number of points used for the local prediction, showing a saturation starting from the cluster sizes of about several tens of points. This fact leads to the conclusion about the spurious finite value of dimension estimates that may follow from processing the data like those shown in Fig. 5 and, hence, points to the stochastic origin of the time series.

2.2.6. Rytov–Dimentberg criterion

Fig. 7 shows the results of calculating the probability distribution functions for the instantaneous amplitude squared of low (left) and high (right) amplitude microseisms. The plots are characterized by monotonically decreasing distribution functions for both low and high amplitude data. We note that for noise-induced oscillations considered in [12] the same behavior was observed for different intensities of the noise, whereas for chaotic oscillations in the same model the situation was qualitatively different, i.e. several well-defined maxima appear in the probability density function. This result can be considered as a convincing argument in favor of the hypothesis that microseism oscillations are either a noise passed through a nonlinear filter or noise-induced oscillations. If the data are filtered noise then the Duffing oscillator [26] influenced by the additive noise can be considered as a good candidate for modeling purposes. Another case is if the data are noise-induced oscillations, which is a result of a noise-induced phase transition that manifests itself in the excitation of noise-induced oscillations. In this case, another oscillator model, like, e.g., a pendulum with a randomly vibrated suspension axis [12], can be used.

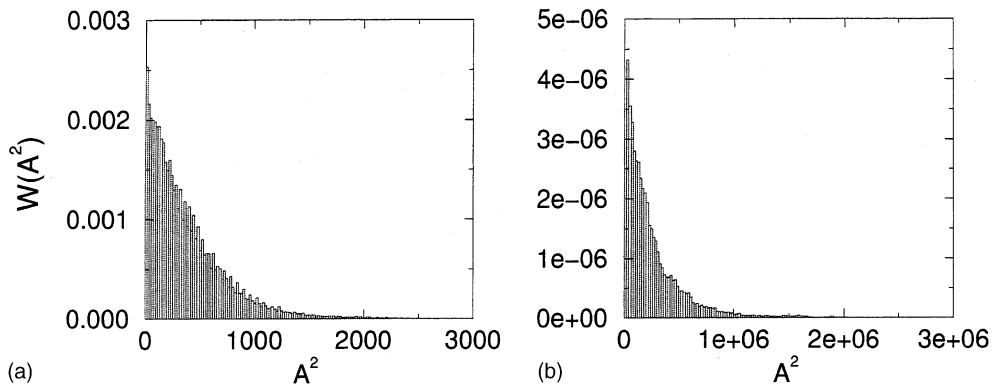


Fig. 7. RD criterion applied to the high amplitude (a) and low amplitude (b) microseisms. The probability distribution function $W(A^2)$ for the instantaneous amplitudes squared decreases monotonically.

3. Analysis of surrogates

The set of both RP and ARMA surrogate data present the same characteristics as the original time series from the viewpoint of correlation dimension analysis. This fact supports the conclusion derived from DVS and Rytov–Dimontberg (RD) tests about the stochastic origin of the studied time series and, therefore, spurious finite value of correlation dimension found in some of our calculations. Like in many other cases discussed in the literature (see e.g., [13,16]), the curves of the local slope of correlation integral for surrogates look very similar to those shown in Fig. 5. We do not reproduce them here, since they do not provide any new information on the studied data. Instead, we would like to discuss in some detail the results of numerical experiments with NLFO surrogates.

In order to simulate the observed characteristics of microseism time series, we adopted as a first step a reductionism point of view. We derived a toy model, that is, a mathematical system that reproduces some characteristics of observations (independently of the physics of the process), in an attempt to concentrate on the global properties of the underlying geophysical system, without paying much attention to the details of real processes. Following the classical assumption that considers microseism time series as a superposition of oscillations, we propose a forced, damped, nonlinear oscillator with additive noise as a working model

$$\begin{aligned} \dot{q} &= p \\ \dot{p} &= -\frac{\partial V(q)}{\partial q} - \delta p + \sum_{i=1}^2 \gamma_i \cos(\omega_i t) + \mu F(t) \end{aligned} \quad (1)$$

where q stands for the displacement, δ the coefficient of damping, V the potential (defined in the Appendix A), γ_i the amplitudes of the external harmonic forces, $F(t)$ white noise and μ its corresponding amplitude. Initially we considered the harmonically excited Duffing oscillator (NLFO) [26], to which Eq. (1) reduces for $i = 1$, $\mu = 0$ and V a bistable potential. In this way, Longuet-Higgins model [2], consisting in an external harmonic force originated by oceanic storms, is preserved, and the nonlinear terms are all included in the potential V . For comparing the time series generated by the nonlinear oscillator with real microseism time series, both in time and frequency domains, two external forces were needed to account for the spectral peaks of ~ 0.1 , ~ 0.2 and ~ 0.016 Hz present in the microseism spectra. A comparative study of the spectral characteristics of microseisms with those of NLFO surrogates, suggested the need to incorporate an n -well potential (NLFO-N) instead of the two-well one with the bistable potential.

In Fig. 8 we present an example of the time series generated by model (1) and in Fig. 9 its corresponding power spectrum. The following parameters (see Appendix A) have been used to generate the time series:

potential : number of wells $n = 11$, $a = 0.5$, $b = 4.0$, $c = 2.0$

friction : $\delta = 0.1$

external force : $\gamma_1 = 20$, $f_1 \equiv \frac{2\pi}{\omega_1} = 0.01$ Hz, $\gamma_2 = 20$, $f_2 \equiv \frac{2\pi}{\omega_2} = 0.25$ Hz

additive white noise : $\mu = 100$

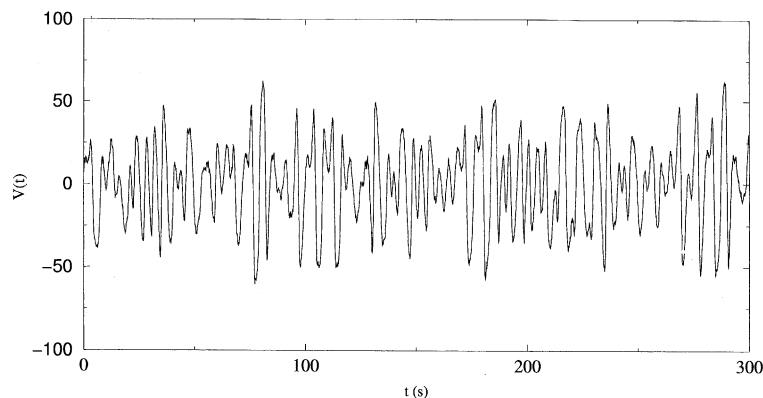


Fig. 8. An example time series generated by the nonlinear oscillator (1) with additive noise ($\mu \neq 0$).

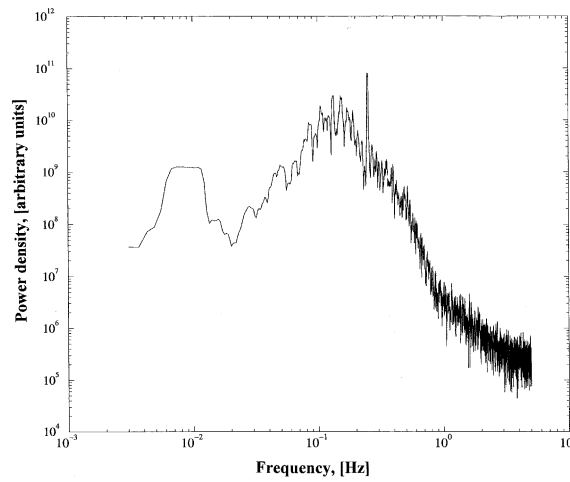


Fig. 9. Power spectrum of the time series shown in Fig. 8.

By comparing Figs. 8 and 9 with Figs. 1a and 2, we can observe that they are qualitatively very similar. For different values of the parameters and different levels of noise, we have found that this model is able to reproduce the spectral characteristics of microseism time series for both high amplitude and low amplitude microseisms, the differences between high and low amplitude depending only on the amplitude of noise μ .

We have applied the same set of time series analysis tests to the generated data. As an example, we present the results of the analysis for a time series generated from Eq. (1) with the above values of the parameters. The results of the tests are the following:

Mutual information. Presents a minimum at 1.3 s, as displayed in Fig. 10, bottom, the curve for $m = 2$.

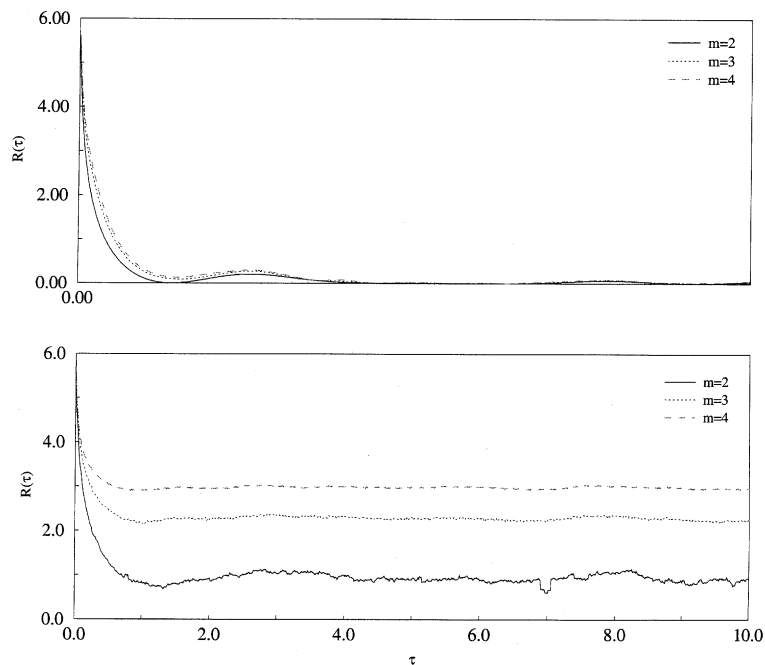


Fig. 10. Redundancies for the time series generated by the system (1). Linear (top) and general, or nonlinear (bottom) redundancy plots for three values of the embedding dimension: $m = 2, 3, 4$. The nonlinear redundancy for the embedding dimension $m = 2$ corresponds to the mutual information.

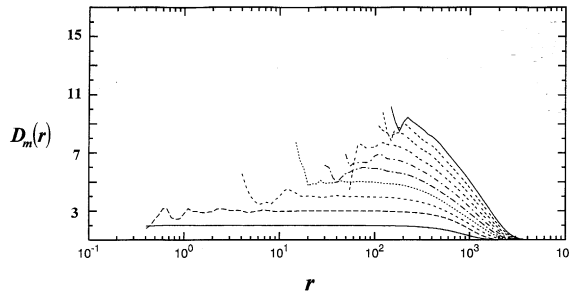


Fig. 11. Local slope of the correlation integral $C_m(r)$ versus the distance r for the embedding dimension changing from $m = 2$ to $m = 11$ for the nonlinear oscillator time series.

Redundancy. Fig. 10 also shows the curves of linear and general redundancy for different values of embedding dimension. The plots show no apparent differences, that should be in the case of a strong noise component.

Correlation dimension. There is a well-defined plateau for low dimensions ($m \leq 8$), see Fig. 11. There is no saturation of the correlation dimension, indicative of the stochasticity of the time series.

DVS (Fig. 12). For an embedding dimension $m = 2$ the prediction error function is monotonically decreasing until reaching a constant value, about in the same manner as it was in the case of microseism data. However, for dimensions $m = 4, 6, 8$, the function displays a local minimum corresponding to a cluster size of about 500 points, indicating better prediction quality for smaller clusters and, therefore, possible presence of determinism in the system. It is however not surprising, since the system at hand is indeed a deterministic oscillator, although perturbed by the noise.

RD criterion. Fig. 13 shows the RD criterion applied to the oscillator time series. The probability density of the square of the instantaneous amplitude presents three low peaks for $A^2 < 500$. These peaks, along with the local minimum in the prediction in the DVS test, indicate a deterministic component in the oscillator, contrary to the results of calculations performed for the microseism data.

By comparing Figs. 1a and 2 relative to microseisms with Figs. 8 and 9 relative to the nonlinear oscillator, we conclude that the model mimics quite well the spectral characteristics of the observed microseisms. As for DVS and RD criteria, the nonlinear oscillator model presents the properties quite different from those of microseism oscillations. It can be, therefore, concluded that low-dimensional models, even with strong noise source included, cannot be used for an adequate mathematical description of the microseism phenomenon. It is worth noting that in attempting to reproduce the characteristics of a time series by means of nonlinear models, the solution may not be unique: different models can reproduce the same observations. We however believe that the model (1) possesses almost all typical properties of low-dimensional nonlinear oscillators, and, hence, the simulation with any other nonlinear oscillator would bring approximately the same results.

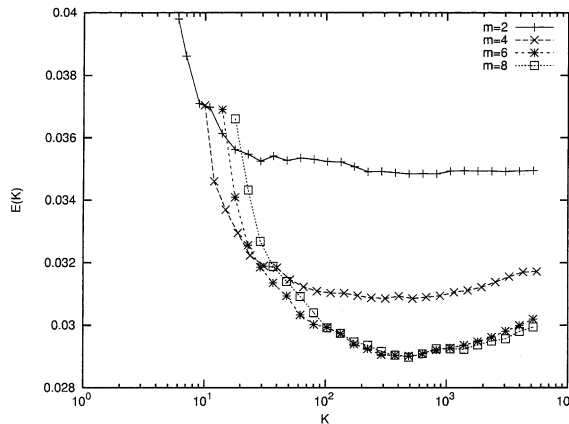


Fig. 12. DVS test for the nonlinear oscillator (1) with additive noise source. The dependence of normalized prediction error $E(k)$ on the cluster size (number of points k) used in deriving the linear predictors in the reconstructed phase space.

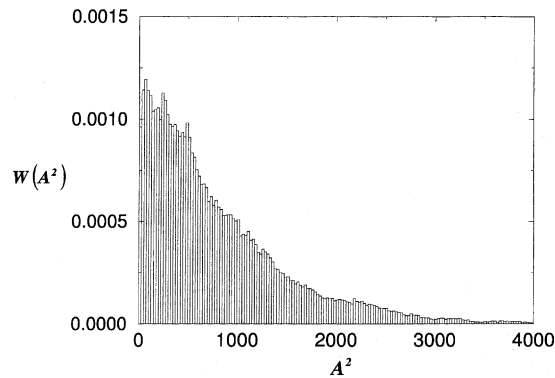


Fig. 13. RD criterion for the nonlinear oscillator. The probability distribution function $W(A^2)$ for the instantaneous amplitudes squared shows well-pronounced maxima at low values of A^2 .

4. Discussion and conclusions

The analysis of microseism time series has revealed some interesting characteristics: time series appear to be stochastic without any indication of nonlinearity and/or determinism. At the same time, up to our knowledge, the models of microseism generation being discussed in the literature [2,6,27,28] are intrinsically nonlinear (two waves interaction mechanism). It should be however noted, that the conventional microseism models developed in the above works were proposed mainly for explaining the shape of power spectra and the analysis of seismic waves propagation, earthquake detectability, etc. (see e.g., the review [3]), and did not focus on the nonlinear properties of data.

In this work we make an attempt to look at the microseism phenomenon from a basically different viewpoint, by considering the geophysical system consisting of atmosphere, ocean and solid earth at the global scale and behaving as an aggregate nonlinear dynamical system that generates microseism oscillations as a result of its complicated dynamics. Such an approach is close in spirit (e.g., from the point of view of the time series analysis), to the study of fully developed turbulent flow in hydrodynamics, when a scalar time series, say, of the amplitude of fluid velocity, is measured at some point to extract qualitative information of the extended multidimensional system. In such a situation, the spectral characteristics based on the notion of waves (or linear modes) are no longer adequate for the description of dynamics [29], and the invariants like correlation dimension or the spectrum of Lyapunov exponents have been suggested to be more appropriate. To get a deeper insight on the dynamics of microseisms, we have performed an analysis of microseism time series from the point of view of dynamical systems, in an attempt to determine whether they are linear or nonlinear, deterministic or stochastic. It should be noted here that, in fact, the question of whether a given time series is deterministic and/or nonlinear has no unambiguous answer, because the result of calculation for any dynamical invariant can be dependent on many external and internal factors, like noise, interaction with other systems not included into consideration, and intrinsic parameters of the calculation procedure. That is why the only meaningful way of analysis seems to be via comparison of the experimental data to some kind of artificial (or surrogate) time series with well-controlled statistical properties [8,15,30].

We have analyzed microseism time series recorded at the eastern Pyrenees on a broadband seismic station located at about 50 km of the shore of the Mediterranean Sea. Microseism power spectra display common typical characteristics for all analyzed microseisms: a broad spectral peak of large amplitude, located at ~ 0.2 Hz, and another broad peak of lower amplitude, located at about 0.1 Hz. An analysis of the time series has displayed strong evidences in favor that the series is purely stochastic without any indication of either determinism or nonlinearity of the process.

Further analysis on records from different geographic origin is needed to establish whether these results are general or are due only local phenomena (our feeling, however, is that these results are of general character). All of the spectral characteristics revealed by the set of tests we have applied to the microseism time series can be quite well reproduced by a forced, dissipative nonlinear oscillator with the presence of additive noise. It has been revealed that the presence of this additive noise is of fundamental importance to mimic all the dynamic features of the microseism time series. It however turned out that the simple nonlinear oscillator model is not capable of reproducing the stochastic properties of the time series analyzed by means of DVS or RD techniques.

A key question, for which there is not yet a definite answer, refers to the nonlinearity of the microseisms time series. Guschin and Pavlenko [31] found some indications of nonlinearity, which was attributed to elastic nonlinearity of sedimentary soils. This interpretation is somewhat ambiguous and raises the question of the similar behavior for low

and high frequency microseisms. A possible solution consists on the assumption that the found nonlinearity is due to multiplicative noise (instead of an additive one), that could be written as $g(q)F(t)$ where $g(q)$ is a nonlinear function of displacements. This aspect will be addressed in a future work.

As it has been pointed out in Section 1, we found it surprising that the spectra of low amplitude microseisms (those generated in the absence of oceanic storms, that is, in the absence of external forces) displayed the same characteristics that the spectra of high amplitude microseisms (those generated by oceanic storms, that is, in the presence of external forces). We simulated this effect by integrating Eq. (1) in the absence of external forces, that is, with only the noise term as a driving force. The shape of the spectrum was found basically the same. The broad spectral peak of large amplitude can now be interpreted as the fundamental harmonic of the potential (that is, a medium property for the case of microseisms), and the broad peak of lower amplitude as a subharmonic of the main frequency. If we interpret the spectral peak of large amplitude as a mechanical resonance of the medium, this resonance could be attributed to a waveguide of 7–8 km thickness, defined by the free surface and Conrad discontinuity. Clearly this interpretation is not contemplated in Longuet-Higgins model. Another model alternative to that of Longuet-Higgins was suggested by Friedrich et al. [28], who attributed the origin of the microseisms generated at the North Sea, and recorded at Graefenberg array, to resonances defined by the geometry of the Fjords.

In applying the RD criterion, we have seen that for the observed microseism time series the probability density function is monotonically decreasing, whereas for the forced oscillator presents some low amplitude peaks. It is worth to note that introducing a narrow-band noise instead of the harmonic forces of the toy model can eliminate the misfit connected with these peaks. At this point we can comment that two extreme possibilities in the model of type (1) that can satisfy observed data can be considered: (i) two harmonic force terms with some amount of additive noise, and (ii) white noise-induced oscillations, without any harmonic force term. In between, any model seems to be possible. As already pointed out, in this first attempt we have chosen the toy model because of its simplicity. The question of the model choice is out of the scope of the present paper and will be addressed in a future work.

Acknowledgements

We would like to thank Prof. P.S. Landa for fruitful discussions. This research has been partially supported by the Direccion General para la Investigacion Cientifica y Tecnologica under grant PB96-0139-C04-02 and INTAS, grant INTAS-952-139. M.U. has been supported by a scholarship of the CIRIT under contract FI/95-1122. V.B.R acknowledges support from JSPS.

Appendix A. The n -well potential

The n -well potential has been constructed under the following conditions: the first derivative should be continuous, whereas the height and broadness of the n -potential wells can be controlled by a few parameters. Although rather arbitrary, for simplicity and symmetry the wells are characterized by a set of $N = (2n + 1)$ parabolas defined as $c(x \pm 2bi)^2$, where c is a parameter and $i = 0, 1, \dots, n$, and another set defined as $c(a - b)/a(x \pm (2i - 1)b)^2 + cb(b - a)$ (see Fig. 14). The two sets of parabolas are joined. The inflection point (that is, the common point) is located at a

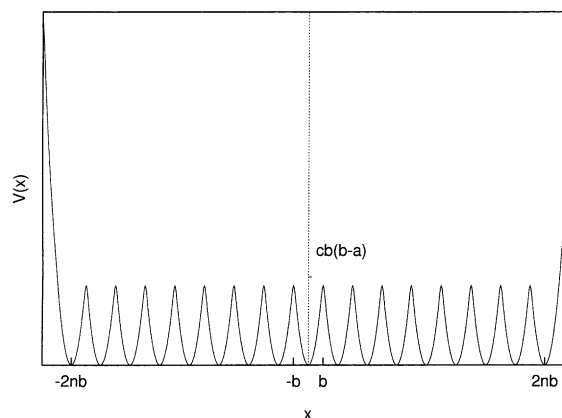


Fig. 14. Geometrical shape of the n -wells nonlinear potential (A.1) used in numerical experiments with system (1).

distance a of the symmetry axis of the parabola. The maximum height of the wells is $cb(b - a)$. The outermost boundaries are of infinite height. So constructed potential function and its first derivative are continuous. If the energy is large enough, the systems oscillates in the broad well that includes many small ones, otherwise in any of the secondary n wells. The equation of the potential is

$$V(x) = \begin{cases} \frac{c(x+2bn)^2}{a} & x < -(2n-1)b - a \\ \frac{c(a-b)}{a}(x + (2n-1)b)^2 + cb(b-a) & -(2n-1)b - a \leq x < -(2n-1)b + a \\ \frac{c(x+2b(n-1))^2}{a} & -(2n-1)b + a \leq x < -(2(n-1)-1)b - a \\ \vdots & \vdots \\ \frac{c(a-b)}{a}(x+b)^2 + cb(b-a) & -b - a \leq x < -b + a \\ \frac{c(a-b)}{a}(x-b)^2 + cb(b-a) & b - a \leq x < b + a \\ \frac{c(a-b)}{a}(x-3b)^2 + cb(b-a) & 3b - a \leq x < 3b + a \\ \vdots & \vdots \\ \frac{c(x-2b(n-1))^2}{a} & (2(n-1)-1)b + a \leq x < (2n-1)b - a \\ \frac{c(a-b)}{a}(x - (2n-1)b)^2 + cb(b-a) & (2n-1)b - a \leq x < (2n-1)b + a \\ \frac{c(x-2bn)^2}{a} & (2n-1)b + a \leq x \end{cases} \quad (\text{A.1})$$

The nonlinearity in the above equation is defined by the potential $\partial V(x)/\partial x$, that is a smooth piecewise continuous function.

References

[1] Aki K, Richards PG. Quantitative seismology. San Francisco: Freeman; 1980.
 [2] Longuet-Higgins MS. A theory for the generation of microseisms. Phil Trans Roy Soc Ser A 1950;243:1–35.
 [3] Webb SC. Broadband seismology and noise under the ocean. Rev Geophys 1998;36:105–42.
 [4] Vila J. The broad band seismic station CAD (Tuner del Cadi, eastern Pyrenees): site characteristics and background noise. Bull Seismol Soc Am 1998;88:297–303.
 [5] Bath M. Introduction to seismology. Stuttgart: Birkhauser Verlag; 1973.
 [6] Kibblewhite AC, Wu CY. The theoretical description of wave–wave interactions as a noise source in the ocean. J Acoust Soc Am 1991;89:2241–52.
 [7] Palus M. Identifying and quantifying chaos by using information-theoretic functionals. In: Weigend AS, Gershenfeld NA, editors. Time series prediction: forecasting the future and understanding the past. SFI studies in the sciences of complexity. Proc. vol. XV. New York: Addison-Wesley; 1993. p. 387–413.
 [8] Schreiber T. Interdisciplinary application of nonlinear time series methods. Phys Repts 1999;308:1–64.
 [9] Marple Jr SL. Digital spectral analysis with applications. New Jersey: Prentice Hall; 1987.
 [10] Fraser AM, Swinney HL. Independent coordinates for strange attractors from mutual information. Phys Rev A 1986;33:1134–40.
 [11] Casdagli MC, Weigend AS. Exploring the continuum between deterministic and stochastic modeling. In: Weigend AS, Gershenfeld NA, editors. Time series prediction: forecasting the future and understanding the past. SFI studies in the sciences of complexity, Proc. vol. XV. New York: Addison-Wesley; 1993. p. 347–66.
 [12] Landa PS, Zaikin AA. Noise-induced phase transition in a pendulum with a randomly vibrating suspension axis. Phys Rev E 1996;54:3535–44.
 [13] Abarbanel HDI, Brown R, Sidorowich JJ, Tsimring LS. The analysis of observed chaotic data in physical systems. Rev Mod Phys 1993;65:1331–92.
 [14] Theiler J, Eubank S, Longtin A, Farmer JD. Testing for nonlinearity in time series: the method of surrogate data. Physica D 1992;58:77–94.
 [15] Schreiber T. Constrained randomization of time series data. Phys Rev Lett 1998;80:2105–8.
 [16] Isliker H, Kurths J. A test for stationarity: finding parts in a time series apt for correlation dimension estimates. Int J Bifurc Chaos 1993;3:1573–83.
 [17] Casdagli M. Recurrence plots revisited. Physica D 1997;108:206–32.
 [18] Takens F. Detecting strange attractors in turbulence. In: Rand DA, Young L-S, editors. Dynamical systems and turbulence. Lecture Notes in Mathematics, vol. 898. Berlin: Springer-Verlag; 1980. p. 336–81.
 [19] Atay FM, Altintas Y. Recovering smooth dynamics from time series with the aid of recurrence plots. Phys Rev E 1999;59:6593–8.
 [20] Grassberger P, Procaccia I. Characterization of strange attractors. Phys Rev Lett 1983;50:346–9.
 [21] Rytov SM. Introduction to statistical radiophysics. Moscow: Nauka; 1966 (in Russian).
 [22] Dimentberg MF. Nonlinear stochastic problems of mechanical oscillations. Moscow: Nauka; 1980 (in Russian).
 [23] Landa PS. Regular and chaotic oscillations. Berlin: Springer; 2001.

- [24] Pikovsky A, Rosenblum M, Kurths J. Synchronization: a universal concept in nonlinear sciences. Cambridge: Cambridge University Press; 2001.
- [25] Ding M, Grebogi C, Ott E, Sauer T, Yorke JA. Estimating correlation dimension from a chaotic time series: when does plateau onset occur? *Physica D* 1993;69:404–34.
- [26] Guckenheimer J, Holmes P. Nonlinear oscillations dynamical systems and bifurcation of vector fields. New York: Springer-Verlag; 1997.
- [27] Keilis-Borok VI. Seismic surface waves in a laterally inhomogeneous earth. Dordrecht: Kluwer; 1989.
- [28] Friedrich A, Krueger F, Klinge K. Ocean-generated microseismic noise located with the Grafenberg array. *J Seismol* 1998;2:47–64.
- [29] Eckman J-P, Ruelle D. Ergodic theory of chaos and strange attractors. *Rev Mod Phys* 1985;57:617–56.
- [30] Theiler J, Prichard D. Constrained realization Monte-Carlo method for hypothesis testing. *Physica D* 1996;94:221–35.
- [31] Guschin VV, Pavlenko OV. A study in nonlinear elasticity based on bispectral characteristics of seismic noise. *Volcanol Seismol* 1998;20:215–29.